

6-8-2024

The Impact of Mechanical Thrombectomy on the Blood-Brain Barrier in Patients With Acute Ischemic Stroke: A Non-contrast MR Imaging Study Using DP-pCASL and NODDI

Nikolaos Mouchtouris

Isaiah Ailes

Ki Chang

Adam Flanders

Feroze Mohamed

See next page for additional authors

Follow this and additional works at: <https://jdc.jefferson.edu/neurosurgeryfp>



Part of the [Analytical, Diagnostic and Therapeutic Techniques and Equipment Commons](#), [Neurology Commons](#), and the [Surgery Commons](#)

[Let us know how access to this document benefits you](#)

This Article is brought to you for free and open access by the Jefferson Digital Commons. The Jefferson Digital Commons is a service of Thomas Jefferson University's [Center for Teaching and Learning \(CTL\)](#). The Commons is a showcase for Jefferson books and journals, peer-reviewed scholarly publications, unique historical collections from the University archives, and teaching tools. The Jefferson Digital Commons allows researchers and interested readers anywhere in the world to learn about and keep up to date with Jefferson scholarship. This article has been accepted for inclusion in Department of Neurosurgery Faculty Papers by an authorized administrator of the Jefferson Digital Commons. For more information, please contact: JeffersonDigitalCommons@jefferson.edu.

Authors

Nikolaos Mouchtouris, Isaiah Ailes, Ki Chang, Adam Flanders, Feroze Mohamed, Stavropoula Tjoumakaris, Michael Gooch, Pascal Jabbour, Robert Rosenwasswer, and Mahdi Alizadeh



The impact of mechanical thrombectomy on the blood–brain barrier in patients with acute ischemic stroke: A non-contrast MR imaging study using DP-pCASL and NODDI

Nikolaos Mouchtouris^{a,*}, Isaiah Ailes^b, Ki Chang^b, Adam Flanders^c, Feroze Mohamed^c, Stavropoula Tjoumakaris^a, Reid Gooch^a, Pascal Jabbour^a, Robert Rosenwasser^a, Mahdi Alizadeh^a

^a Department of Neurological Surgery, Thomas Jefferson University Hospital, Philadelphia, PA, United States

^b Sidney Kimmel Medical College, Thomas Jefferson University, Philadelphia, PA, United States

^c Department of Radiology, Thomas Jefferson University Hospital, Philadelphia, PA, United States

ARTICLE INFO

Keywords:

Blood–brain barrier
Hemorrhagic stroke
Ischemic stroke
Magnetic Resonance Imaging
Thrombectomy

ABSTRACT

Background and purpose: While mechanical thrombectomy (MT) achieves restoration of cerebral blood flow to the area at risk in patients with acute ischemic stroke (AIS), the influx of blood flow may exacerbate the blood–brain barrier (BBB) disruption and extravasation across the BBB, and it therefore remains unclear how reperfusion impacts the blood–brain barrier integrity. In this study, we use diffusion-prepared pseudocontinuous ASL (DP-pCASL) and Neurite Orientation Dispersion and Density Imaging (NODDI) sequence to measure the water exchange rate (k_w) in patients who underwent either MT or medical management and determine its impact on the brain tissue microstructure in order to elucidate the impact of MT on BBB complex integrity.

Materials and methods: We prospectively enrolled 21 patients with AIS treated at our institution from 10/2021 to 6/2023 who underwent MR imaging at a 3.0-Tesla scanner. Patients underwent DP-pCASL and NODDI imaging in addition to the standard stroke protocol which generated cerebral blood flow (CBF), arterial transit time (ATT), water exchange rate (k_w), orientation dispersion index (ODI), intracellular volume fraction (ICVF), and free water fraction (FWF) parametric maps.

Results: Of the 21 patients, 11 underwent MT and 10 were treated non-operatively. The average age and NIHSS for the MT cohort and non-MT cohorts were 69.3 ± 16.6 years old and 15.0 (12.0–20.0), and 70.2 ± 10.7 ($p = 0.882$) and 6.0 (3.8–9.0, $p = 0.003$) respectively. The average CBF, ATT, and k_w in the infarcted territory of the MT cohort were 38.2 (18.4–59.6), 1347.6 (1182.5–1842.3), and 107.8 (79.2–140.1) respectively. The average CBF, ATT, and k_w in the stroke ROI were 16.0 (8.8–36.6, $p = 0.036$), 1090.8 (937.1–1258.9, $p = 0.013$), 89.7 (68.0–122.7, $p = 0.314$) respectively. Linear regression analysis showed increasing CBF ($p = 0.008$) and undergoing mechanical thrombectomy ($p = 0.048$) were significant predictors of increased k_w .

Conclusion: Using our multimodal non-contrast MRI protocol, we demonstrate that increased CBF and mechanical thrombectomy increased k_w , suggesting a better functioning BBB complex. Higher k_w suggests less disruption of the BBB complex in the MT cohort.

1. Introduction

The management of acute ischemic stroke (AIS) has been revolutionized in the past decade with the widespread adoption of mechanical

thrombectomy (MT). The indications for mechanical thrombectomy have drastically expanded, now including large (Berkhemer et al., 2015) and medium (Menon et al., 2019) vessel occlusions as well as patients with wake-up strokes (Nogueira et al., 2018) and large ischemic core

Abbreviations: AIS, acute ischemic stroke; MT, mechanical thrombectomy; HT, hemorrhagic transformation; BBBP, blood–brain barrier permeability; DP-pCASL, diffusion-prepared pseudocontinuous ASL; NODDI, Neurite Orientation Dispersion and Density Imaging; ATT, arterial transit time; k_w , water exchange rate; ICVF, intracellular volume fraction; FWF, free water fraction; ODI, orientation dispersion index; AQP4, aquaporin-4.

* Corresponding author at: Thomas Jefferson University Hospital, 909 Walnut St, 3rd floor, Philadelphia, PA, 19107, United States.

E-mail address: Nikolaos.Mouchtouris@jefferson.edu (N. Mouchtouris).

<https://doi.org/10.1016/j.nicl.2024.103629>

Received 18 April 2024; Received in revised form 23 May 2024; Accepted 4 June 2024

Available online 8 June 2024

2213-1582/© 2024 The Author(s). Published by Elsevier Inc. This is an open access article under the CC BY-NC license (<http://creativecommons.org/licenses/by-nc/4.0/>).

volumes (Costalat et al., 2024; Sarraj et al., 2023). Despite the favorable functional outcomes after thrombectomy, symptomatic hemorrhagic transformation (HT) remains a debilitating adverse event that occurs in up to 10 % of patients (Mouchtouris et al., 2019; Fiorelli et al., 1999; Strbian et al., 2011; Andrews et al., 2019).

The initial ischemic insult disrupts the blood–brain barrier (BBB), leading to increased blood–brain barrier permeability (BBBP). The increased permeability results in extravasation of blood and inflammatory cells across the barrier, which predisposes patients to hemorrhagic transformation (Spronk et al., 2021; Arba et al., 2021). Revascularization achieves restoration of cerebral blood flow to the area at risk with resolution of ischemia and improvement of stroke symptoms. However, the influx of blood flow may exacerbate the extravasation across the BBB, and it is therefore unclear how the reperfusion impacts the blood–brain barrier integrity.

Novel neuroimaging techniques have enabled the mapping of the BBB complex and quantifying its permeability. Diffusion-prepared pseudocontinuous ASL (DP-pCASL) is a sequence that quantifies BBBP by magnetically labeling water molecules and tracking their movement across the blood–brain barrier (Shao et al., 2019), calculating the water exchange rate (k_w) (Shao et al., 2019; Wang et al., 2012; Shao et al., 2020; Ling et al., 2023; Ford et al., 2022; Uchida et al., 2022; Uchida et al., 2023; Uchida et al., 2023; Uchida et al., 2024). The transport of water across the BBB is mediated by three main processes: passive diffusion, active co-transport through the endothelial membrane, and predominantly facilitated diffusion through the dedicated water channel aquaporin-4 (AQP4). Located on the astrocytic end foot that forms part of the BBB complex, AQP4 is initially downregulated during the early stages of ischemic stroke followed by upregulation and involvement in vasogenic edema clearance (Abbott et al., 2006; Howarth, 2014). Early studies have validated DP-pCASL in a few CNS pathologies (Ford et al., 2022) in humans, including one study in patients with ischemic stroke (Mouchtouris et al., 2024) as well as in animal stroke model (Tiwari et al., 2017), showing a trend of decreased k_w in pathological states. However, it has not been studied in patients undergoing mechanical thrombectomy with rapid reperfusion of the territory at risk. Additionally, Neurite Orientation Dispersion and Density Imaging (NODDI) is a diffusion-based sequence that has been used to measure the ischemic burden on parenchymal microstructure and has the potential to quantify the cytotoxic and vasogenic edema in this patient population.

In this study, our goal is to determine the k_w derived from DP-pCASL

in AIS patients treated either with MT or non-operatively and identify its predictors. We also use NODDI to better understand the impact of mechanical thrombectomy on the various tissue compartments surrounding the BBB complex. We hypothesize that patients who are treated non-operatively have decreased k_w within the infarct when compared to those undergoing mechanical thrombectomy with successful recanalization. We believe that this work will elucidate the impact of restoring cerebral blood flow on the integrity of the blood–brain barrier in an effort to minimize hemorrhagic conversion and optimize functional recovery.

2. Materials and methods

2.1. Patient selection and variables

The study protocol was approved by the University Institutional Review Board (#21D.100). Written consent from patients or their surrogate was required to participate in the study. The STROBE guidelines for an observational case-control study were followed. We prospectively enrolled 21 patients with AIS treated at our institution from 10/2021 to 6/2023 who underwent MR imaging at a 3.0-Tesla MRI scanner (Fig. 1). The inclusion criteria were: older than 18 years old, diagnosed with a supratentorial ischemic stroke, able to undergo a 3.0T MRI. The exclusion criteria were: imaging was negative for ischemic stroke, having an implant not compatible with the 3.0T MRI, and unable to tolerate the imaging resulting in motion artifact. Due to strict eligibility criteria, the patients enrolled were not consecutive patients. From those enrolled, patients were grouped into two cohorts: those who underwent mechanical thrombectomy and those treated non-operatively. Data regarding patient demographics, clinical presentation, time from symptom onset, presence of vascular risk factors, relevant antiplatelet and anticoagulant medications, stroke treatments, such as intravenous alteplase or tenecteplase, and mechanical thrombectomy, and functional outcomes were collected. Stroke severity was measured using the National Institutes of Health Stroke Scale (NIHSS) on admission. The success of recanalization of the acute occlusion after mechanical thrombectomy is determined using the modified Treatment in Cerebral Infarction (mTICI) scale, ranging from 0 to 3. Zero means no recanalization, 1 is minimal recanalization, 2a is recanalization of less than half of the branches of the occluded vessel, 2b is recanalization of more than half of the branches of the occluded vessel, 2c is near-complete

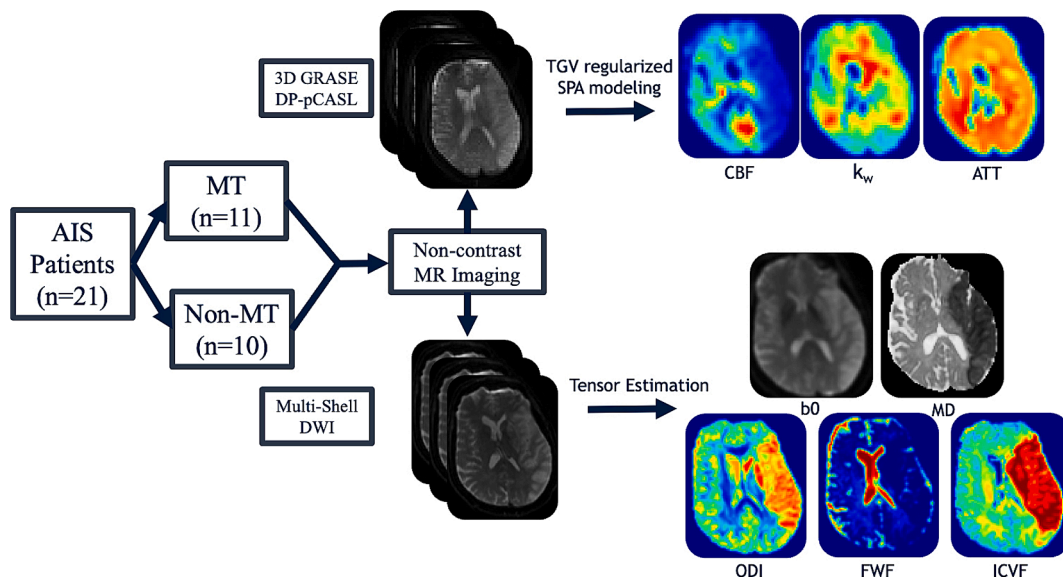


Fig. 1. Patient enrollment workflow and post-acquisition imaging processing methodology for the DP-pCASL and NODDI sequences and their derived parametric maps.

recanalization, and 3 is complete recanalization. Functional outcome is reported using the modified Rankin scale (mRS), ranging from 0 to 6 with 0 being neurologically intact to 6 being deceased. Data analysis was conducted after removal of identifiable personal health information.

2.2. Imaging sequences and acquisition

All scans were performed on a 3.0T Siemens MRI scanner with a dedicated 64-channel head and neck coil. Participants underwent the following MRI sequences: high-resolution T1 without contrast, T2, fluid-attenuated inversion recovery imaging (FLAIR), susceptibility weighted imaging (SWI), NODDI, and diffusion-prepared pseudocontinuous arterial spin label (DP-pCASL) sequence. The NODDI sequence is used in this project to generate the diffusion sequences b_0 and mean diffusivity (MD), intracellular space (ICVF), extracellular space (ODI), and the fraction of free water (FWF) parametric maps. This sequence helps quantify diffusivity in the various tissue compartments in patients with AIS. DP-pCASL is used to generate the cerebral blood flow (CBF), arterial transit time (ATT), and k_w parametric maps (Fig. 1).

The ASL imaging was performed with a diffusion preparation module with spoiling of non-Carr-Purcell-Meiboom-Gill (CPMG) signals integrated with pseudo-continuous ASL (pCASL) and 3D gradient and spin echo (GRASE) readout. The tissue/capillary fraction of the ASL signal was separated by appropriate diffusion weighting ($b = 50 \text{ s/mm}^2$). Water extraction rate (k_w) was quantified using a single-pass approximation (SPA) model with total generalized variation (TGV) regularization. The DP-pCASL imaging parameters were: voxel size of $3.5 \times 3.5 \times 8.0 \text{ mm}^3$, TR = 4.2 s, TE = 36.2 ms, FOV = 224 mm, 12 slices + 10 % oversampling, labeling duration = 1.5 s, $b = 0 \text{ s/mm}^2$ and 14 s/mm^2 for post-labeling delay (PLD) of 0.9 s with 15 measurements, $b = 0 \text{ s/mm}^2$ and 50 s/mm^2 for PLD of 1.8 s with 20 measurements, and total scan time = 10 mins. The parameters for the NODDI scan are the following: voxel size $1.8 \times 1.8 \times 2.0$, 2-shell diffusion scans ($b = 1000 \text{ s/mm}^2$, $b = 2800 \text{ s/mm}^2$), 64 directions of diffusion signal per shell, and 4 reference scans (b_0) for motion correction. Acquisition time was 12 min. The parameters for the T1-weighted imaging used were: FOV = 25.5 cm, voxel size = $0.9 \times 0.9 \times 1.0 \text{ mm}^3$, matrix size = 288×288 , TR = 2.2 s, TE = 2.49 ms and slice thickness = 1 mm.

2.3. Post-acquisition imaging processing

Post-acquisition imaging processing of the DP-pCASL sequence (Fig. 1) was performed by first obtaining the raw imaging data in.dat format from the 3.0T scanner, then carrying out motion correlation, coregistration to T1, and skull stripping. Then, single-pass approximation modeling was used with the total generalized variation (TGV) regularization algorithm to generate the CBF, ATT, and k_w parametric maps. CBF is reported in ml/100 g/min, ATT in milliseconds (ms), k_w in 1/minutes (min^{-1}). A Gaussian filter with a full-width at half maximum (FWHM) of 5 mm was applied. The Water exchange rate quantification toolbox (v1.0) developed by Shao et al was utilized to perform this processing (Shao et al., 2019).

The NODDI diffusion volumes were preprocessed for eddy current distortion and motion correction using FSL (<https://fsl.fmrib.ox.ac.uk>). For this project, only mean diffusivity (MD) was used from diffusion tensor estimate and FWF, ICVF and ODI were calculated from NODDI estimation using NODDI Matlab toolbox (<http://mig.cs.ucl.ac.uk/index.php?n=Tutorial.NODDIatlab>). Additionally, averaged diffusion reference scan (b_0) was used in this analysis.

Entropy was calculated for all the parametric maps generated from DP-pCASL and NODDI using the functionality 'entropy for grayscale images' through Matlab's Image Processing Toolbox that calculates the probability distribution of pixel intensities.

2.4. Stroke segmentation and registration

Stroke segmentation was performed using ITK-SNAP's Automatic Segmentation functionality. The infarcted territories were segmented based on the diffusion b_0 maps and manually verified by the first author against the MD map that is derived from diffusion tensor model. The stroke mask used as region-of-interest (ROI) throughout the analysis. We generated 21 stroke masks, each representing each of the 21 patients' strokes. We then flipped these masks to generate the mirror-images of the stroke masks, representing the contralateral, unaffected, hemisphere of each patient using the 'flip-image' functionality from Medical Image Registration Toolkit (MIRTK) (Rueckert et al., 1999). Lastly, the diffusion b_0 -derived stroke masks of each of the 21 patients were coregistered onto the corresponding PLD2000 M0 volume of DP-pCASL sequence using the FSL's FMRIB's Linear Image Registration Tool (FLIRT) (Jenkinson et al., 2002) in order to transform the stroke ROI onto the DP-pCASL space. The mean signal intensity and entropy of each ROI were calculated from all parametric maps generated from DP-pCASL and NODDI.

2.5. Statistical analysis

Data is presented as mean and standard deviation (SD) for continuous variables that are normally distributed and median and interquartile range (IQR) for non-normally distributed variables. Categorical variables are presented with count and frequency. The comparison of patient and imaging characteristics were performed using χ^2 and Fisher's Exact for categorical variables and Mann-Whitney U for nonparametric continuous variables. Dimensionality reduction and data visualization was performed using principal component analysis (PCA) for all continuous variables. Lastly, all of the continuous variables were converted to z-scores to control for outliers and were added into a backward linear regression analysis with k_w as the dependent continuous variable. R , R^2 , Durbin-Watson, Akaike information criterion (AIC) and variance inflation factors (VIF) were used to determine the optimal regression model. Statistical significance was achieved when p-value is < 0.05 . The univariable and multivariable regression analyses were carried out with IBM SPSS (Version 26.0. Armonk, NY: IBM Corp.). Dimensionality reduction, data visualization and partial correlation analyses were carried out in Python.

3. Results

3.1. Patient demographics and clinical characteristics

A total of 21 patients with supratentorial ischemic strokes were studied, of whom 11 (52.4 %) underwent mechanical thrombectomy and 10 (47.6 %) were managed non-operatively. The mean age of the overall cohort of patients was 69.7 ± 13.8 . The patient cohort included 12 (57.1 %) men and 9 (42.9 %) women with a median admission NIHSS of 12.0 (5.0–19.0). The median infarct volume was 23.9 ml (8.0–93.1). The median time between symptoms and MRI was 56.3 h (24.2–146.4). Four (19 %) patients received alteplase on admission. Hemorrhagic conversion occurred in 2 (9.5 %) of patients. The average k_w of the entire cohort was 103.6 ± 34.0 , the average k_w in the 2 patients with HT was 127.9 ± 28.5 while the average k_w in those without HT was 101.1 ± 34.1 ($p = 0.306$). The average mRS score at discharge was 3.0 (1.5–4.0) with 10 (47.6 %) of patients achieving a favorable functional outcome (mRS 0–2).

3.2. Mechanical thrombectomy (MT) cohort

Eleven patients underwent mechanical thrombectomy for their acute ischemic stroke, of whom 6 (54.5 %) were men and 5 (45.5 %) were women (Table 1). The average age and NIHSS on admission were 69.3 ± 16.6 years old and 15.0 (12.0–20.0) respectively. Of the 11, 6 (54.5 %)

Table 1
Patient characteristics and clinical presentation.

	Overall Cohort (n = 21)	Thrombectomy Cohort (n = 11)	Nonoperative Cohort (n = 10)	p-value
Age, years ± SD	69.7 ± 13.8	69.3 ± 16.6	70.2 ± 10.7	0.88
Sex				
Male	12 (57.1 %)	6 (54.5 %)	6 (60 %)	1.00
Female	9 (42.9 %)	5 (45.5 %)	4 (40 %)	
NIHSS	12.0 (5.0–19.0)	15.0 (12.0–20.0)	6.0 (3.8–9.0)	0.003
Infarct Volume, ml	23.9 (8.0–93.1)	66.7 (7.1–103.0)	19.6 (8.1–38.5)	0.43
Time from Symptoms to MRI	56.3 (24.2–146.4)	48.5 (24.0–94.7)	70.2 (25.8–237.4)	0.47
Stroke Laterality				
Left hemisphere	10 (47.6 %)	4 (36.4 %)	6 (60 %)	0.40
Right hemisphere	11 (52.4 %)	7 (63.6 %)	4 (40 %)	
Alteplase/Tenecteplase	4 (19.0 %)	2 (18.2 %)	2 (20 %)	1.00
Hemorrhagic Transformation	2 (9.5 %)	1 (9.1 %)	1 (10 %)	1.00
Modified Rankin scale (mRS) at Discharge	3.0 (1.5–4.0)	3.0 (1.0–6.0)	2.5 (1.8–4.0)	0.71
Favorable Functional Status (mRS 0–2)	10 (47.6 %)	5 (45.5 %)	5 (50 %)	1.00

achieved a mTICI 3 reperfusion, 4 (36.4 %) achieved mTICI 2b, and 1 (9.1 %) achieved mTICI 2a. The median infarct volume was 66.7 ml (7.1–103.0). All patients underwent MR imaging after mechanical thrombectomy at an average of 48.5 (24.0–94.7) hours from symptom onset. Two of them (18.2 %) received intravenous alteplase on arrival. HT occurred in 1 (9.1 %) patient. The average k_w intensity and entropy in the stroke ROI of the MT cohort was 107.8 (79.2–140.1). The average intensity and entropy of the stroke ROI for b0, MD, ODI, ICVF, FWF, CBF and ATT are displayed in Table 2.

3.3. Non-operative (Non-MT) AIS cohort

Ten patients that were treated non-operatively for their AIS were included in this cohort, of whom 6 were men (60 %) and 4 were women (40 %). The average age and NIHSS in this cohort were 70.2 ± 10.7 (p = 0.88) and 6.0 (3.8–9.0, p = 0.003) respectively. The median infarct volume was 19.6 (8.1–38.5, p = 0.43). Patients underwent MR imaging at an average of 70.2 (25.8–237.4, p = 0.47) hours from symptom onset. TPA was administered in 2 (20 %) patients and hemorrhagic transformation occurred in 1 (10 %). The average mRS at discharge was 2.5 (1.8–4.0) with 50 % of patients achieving a favorable functional status (mRS 0–2).

The average k_w intensity in the stroke ROI of the non-MT cohort was 89.7 (68.0–122.7, p = 0.31). All of the intensity and entropy values for the stroke ROIs on b0, MD, CBF, ATT, k_w , ODI, ICVF, and FWF of the non-MT cohort are shown in Table 2.

3.4. Multivariable linear regression analysis

A stepwise linear regression analysis was performed with the stroke ROI k_w as the dependent variable and all of the variables on the univariable analysis as the independent variables (Table 3). All continuous variables were converted to z-scores prior to inputting into the regression model. Increasing CBF (standardized beta 0.550, 95 % CI 0.167 to 0.934, p = 0.008) and undergoing mechanical thrombectomy (beta 0.362, 95 % CI 0.009 to 1.442, p = 0.048) were significant predictors of increased k_w (R = 0.784, R² 0.614, Durbin-Watson = 2.098). tPA (beta -0.272, 95 % CI -1.669 to 0.283, p = 0.151), FWF (beta 0.270, 95 % CI -0.078 to 0.618, p = 0.119), and time to MRI (beta 0.270, 95 % CI -0.086 to 0.641, p = 0.125) were also in the final model but did not achieve statistical significance. Fig. 2 shows 4 patients that demonstrate the findings of the linear regression analysis. Patient A is a 77-year old female who underwent MT for right M1 occlusion with TICI 3 recanalization. Her b0 and MD sequences show the right MCA territory infarct, her DP-pCASL scan shows high CBF and high k_w . Her NODDI scan shows heterogenous ODI signal: high ODI anteriorly where k_w is moderate and decreased ODI posteriorly where her k_w is the highest. Patient B is a 95-

Table 2
Comparison of Stroke ROI Parameters between the mechanical thrombectomy (MT) and non-MT cohorts.

Parametric Map	MT Stroke ROIs (n = 11)	Non-MT Stroke ROIs (n = 10)	P-value
b0			
Median Intensity (IQR)	520.8 (468.6–642.1)	425.0 (284.4–693.4)	0.51
Entropy (IQR)	6.61 (6.36–7.00)	6.88 (5.72–7.14)	0.67
Mean Diffusivity × 10 ⁻⁴			
Median Intensity (IQR)	4.5 (4.2–5.3)	4.3 (3.1–5.1)	0.39
Entropy (IQR)	6.32 (6.02–6.75)	6.16 (5.31–6.85)	0.71
ODI			
Median Intensity (IQR)	0.55 (0.45–0.59)	0.57 (0.41–0.62)	0.65
Entropy (IQR)	7.42 (6.36–7.50)	7.24 (4.00–7.44)	0.51
ICVF			
Median Intensity (IQR)	0.66 (0.52–0.75)	0.71 (0.56–0.87)	0.35
Entropy (IQR)	6.80 (5.90–7.29)	4.90 (2.76–6.72)	0.11
FWF			
Median Intensity (IQR)	0.11 (0.07–0.15)	0.06(0.04–0.12)	0.17
Entropy (IQR)	4.36 (2.95–5.33)	3.36 (1.61–4.37)	0.11
CBF (ml/100 g/min)			
Median Intensity (IQR)	38.2 (18.4–59.6)	16.0 (8.8–36.6)	0.036
Entropy (IQR)	6.49 (6.06–6.90)	6.33 (5.12–6.86)	0.56
ATT (ms)			
Median Intensity (IQR)	1347.6 (1182.5–1842.3)	1090.8 (937.1–1258.9)	0.013
Entropy (IQR)	5.99 (5.27–6.18)	5.45 (5.02–6.18)	0.47
k_w (min ⁻¹)			
Median Intensity (IQR)	107.8 (79.2–140.1)	89.7 (68.0–122.7)	0.31
Entropy (IQR)	6.44 (6.14–7.06)	6.03 (5.12–6.84)	0.22

year old female who underwent mechanical thrombectomy for left M1 occlusion with TICI 3 recanalization. Her imaging shows small left corona radiata infarct, moderate ODI, moderate FWF, moderate CBF,

Table 3
Univariable and multivariable linear regression analysis for predictors of increasing k_w .

Variable	Univariable		Multivariable			
	Beta Coefficient	p-value	Standardized Beta Coefficient	Lower Bound 95 % CI	Upper Bound 95 % CI	p-value
Age	0.344	0.126				
tPA	-0.727	0.476	-0.272	-1.669	0.283	0.151
Gender	0.132	0.567				
HT	0.237	0.300				
Thrombectomy	0.223	0.331	0.362	0.009	1.442	0.048
NIHSS	0.048	0.835				
Time to MRI	0.187	0.417	0.277	-0.086	0.641	0.125
Stroke Volume	-0.008	0.972				
b0	0.051	0.827				
MD	0.366	0.103				
ODI	-0.251	0.272				
FWF	0.301	0.185	0.270	-0.078	0.618	0.119
ICVF	-0.401	0.071				
CBF	0.511	0.018	0.550	0.167	0.934	0.008
ATT	0.068	0.769				

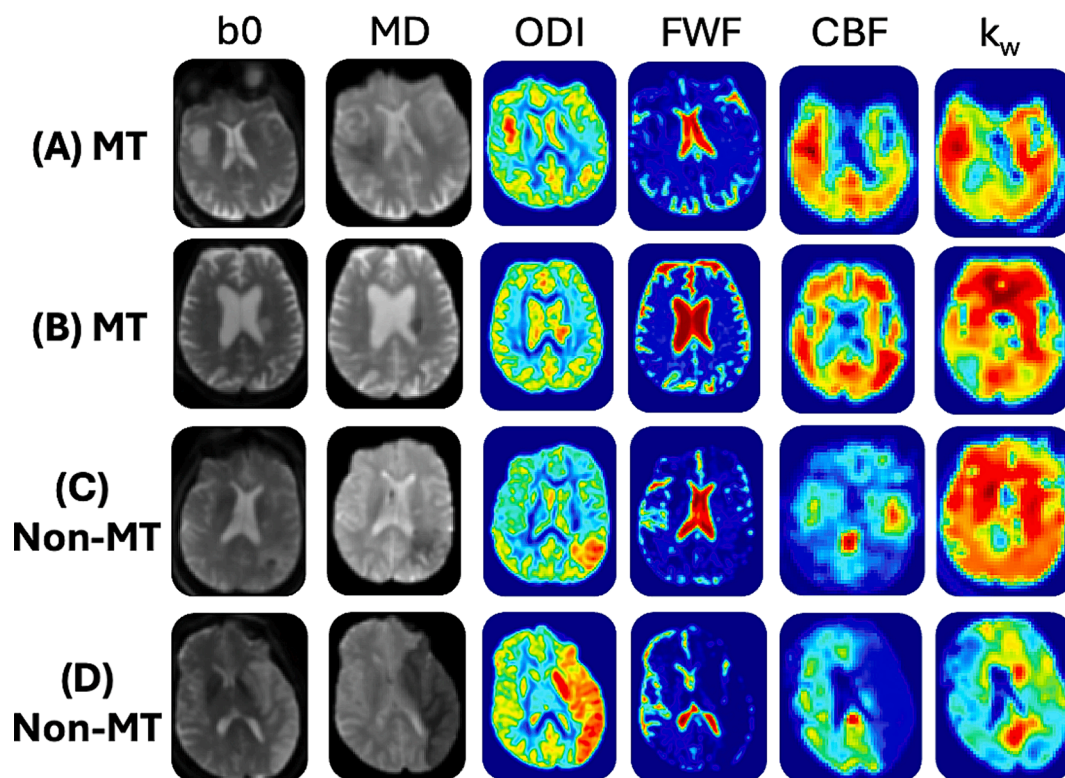


Fig. 2. Key DP-pCASL and NODDI parametric maps from 4 patients showing the variability in the ischemic burden and impact on tissue microstructure after AIS. Patient (A) and (B) underwent mechanical thrombectomy while patients (C) and (D) underwent medical management only for AIS. Patient (A) shows high CBF and high k_w . Patient (B) shows moderate ODI, moderate FWF, moderate CBF, and high k_w . Patient (C) has a left parietal stroke with hemorrhagic transformation with moderate ODI, moderate FWF, decreased CBF, and moderate k_w . Patient (D) had a left MCA stroke with high ODI, low FWF, low CBF and low k_w .

and high k_w . Patient C is 64-year old male with a left parietal stroke that did not meet the criteria for mechanical thrombectomy and was managed non-operatively. His imaging shows mild hemorrhagic transformation with moderate ODI, moderate FWF, decreased CBF, and moderate k_w . Patient D is a 76-year old male also managed medically with a large left MCA infarct with high ODI, low FWF, low CBF and low k_w .

4. Discussion

While the rates of successful MT are high, the resultant ischemic burden and vasogenic edema continue to significantly complicate

recovery in many patients, oftentimes requiring a decompressive hemicraniectomy for malignant cerebral edema and prolonged ICU hospitalization (Grefkes and Fink, 2020; Huang et al., 2019; Wang et al., 2021). The impact of recanalization on the brain parenchyma microstructure and the extent of cytotoxic and vasogenic edema depends on the integrity of the BBB after AIS, which remains unclear. In this study, we used two non-contrast MRI sequences, DP-pCASL and NODDI, to quantify the BBBP in patients undergoing MT compared to medical management for AIS. DP-pCASL uses perfusion-based measures to calculate the water exchange rate across the BBB, while NODDI measures the ischemic burden as well as the diffusivity in various compartments surrounding the BBB complex.

DP-pCASL is a non-contrast MRI sequence that measures the water exchange rate across the BBB and serves as the ideal marker for BBB disruption in this patient population. More specifically, water exchange across the BBB occurs predominantly based on the aquaporin-4 channel (AQP4) which plays an important role in stroke. The AQP4 channel is downregulated in the early phases of AIS but gets upregulated in a delayed fashion (Ribeiro et al., 2006; Datta et al., 2022). Our study corroborates the decreased water exchange rate seen in patients with AIS in comparison to healthy controls (Shao et al., 2024; Mouchtouris et al., 2024), which is consistent with the AIS-induced BBB disruption and early downregulation of AQP4. Interestingly, the non-MT cohort had a lower k_w than the MT cohort, whose values were comparable to the age-matched healthy volunteers studied in Shao et al. (Shao et al., 2024). This finding suggests that successful reperfusion to a territory at risk minimizes the ischemic insult to the BBB complex, preserving its integrity and ability to transport molecules across it. It appears that recanalization maintains k_w at physiologic levels, whereas persistent vessel occlusion as seen in the non-MT cohort results in a pathologic decrease in k_w . Measuring k_w can therefore provide useful insight into the stroke recovery process.

4.1. Relationship between CBF, MT, and k_w

Our multivariable linear regression analysis showed that increasing CBF and undergoing mechanical thrombectomy were significant predictors of increased k_w . MT achieves rapid recanalization and reperfusion of the cerebral territory at risk, which has an unclear impact on the BBB complex. While reperfusion may eliminate the ischemic insult and reduce the oxidative stress, there is concern that the restoration of blood flow may aggravate the BBB disruption by enabling extravasation of inflammatory cells and cytokines through the BBB complex and into the parenchyma. Neutrophils and macrophages are recruited to the injured BBB and extravasate into the parenchyma through the degraded tight junctions. During their activation and recruitment, neutrophils secrete pro-inflammatory cytokines and MMPs, MMP-2 and MMP-9 in particular, which aggravate the BBB permeability by further degrading the tight junctions and allowing for further immune cell infiltration into the parenchyma (Sarvari et al., 2020; Spronk et al., 2021). Peripheral immune cell infiltration causes neurotoxicity and further neuronal damage. The hypoxic event also leads to reactive oxygen species (ROS) formation, which exacerbates all of the aforementioned processes, endothelial damage, neutrophil and macrophage activation, and neurotoxicity (Mo et al., 2020). In our study, increasing CBF was a significant predictor of increasing k_w , suggesting less disruption to the BBB complex with intact transport mechanisms in patients with higher CBF to the infarcted area (Sandoval and Witt, 2008). Our findings suggest that achieving recanalization and restoration of blood flow with mechanical thrombectomy is strongly associated with restoration of BBB complex integrity and return of the water exchange rate to healthy levels.

The time interval from symptom onset to MRI is known to play a role in BBB permeability in patients after ischemic stroke (Sandoval and Witt, 2008; Bernardo-Castro et al., 2020). In our study, this time interval was not significantly different in the univariable analysis between the two cohorts. Given the known role of time on BBBP from existing literature, we included time to MRI in the multivariable analysis, however it still did not significantly impact k_w . Our patients were all scanned during the acute phase of their recovery, which is why the impact of time is not evident. Larger scale studies that include patients with acute, subacute, and chronic strokes will better elucidate the impact of time from symptom onset to MRI on k_w .

Our study entails several limitations that need to be taken into consideration. The MT cohort consisted of patients with higher stroke severity and large vessel occlusions that warranted a MT, while only a small portion of the non-operative cohort had a large vessel occlusion. For that reason, there is a significant difference in the NIHSS on

admission as well as varying pathophysiology of the underlying stroke etiology. Many patients admitted with ischemic stroke had implanted devices (e.g. pacemakers, cerebral or cardiac stents, etc.) that were not compatible with the 3T MRI scanner, some patients were scanned but had to be excluded due to motion artifact, while others were excluded for having infratentorial strokes, resulting in our small sample size. Further, the average k_w in those with HT was higher than those without HT, however, it did not reach significance given that only 2 out of 21 patients had HT. For that reason, HT was excluded from the regression model and correlating it with k_w was beyond the scope of this study. Additionally, the ATT was significantly longer in the MT cohort than the non-MT cohort, which is counterintuitive given that recanalization should decrease the transit time. However, non-MT patients have a significant compensatory hypertensive response driven by cerebral autoregulation to increase perfusion after stroke (Semplicini et al., 2003; Qureshi, 2008), while MT patients are maintained normotensive to minimize the risk of HT postoperatively. The impact of blood pressure on ATT and k_w in this patient population requires further investigation. Lastly, the medical complexity and heterogeneity of this patient population poses a significant challenge when studying DP-pCASL in patients who underwent MT versus those who were treated non-operatively, which is why we use a multivariable regression analysis to control for the differences between the two cohorts studied.

5. Conclusions

Mechanical thrombectomy has revolutionized the treatment of acute ischemic stroke in the past decade, however, it remains unclear how the reperfusion of an infarcted territory impacts the blood-brain barrier and whether it increases the risk of hemorrhagic transformation. Using the non-contrast MRI sequences DP-pCASL and NODDI, we demonstrate that increased CBF and undergoing mechanical thrombectomy increased k_w , suggesting a better functioning BBB complex. Our study corroborates the potential of DP-pCASL in this patient population to improve functional outcomes and recovery from ischemic stroke.

CRedit authorship contribution statement

Nikolaos Mouchtouris: Writing – review & editing, Writing – original draft, Supervision, Formal analysis, Data curation, Conceptualization. **Isaiah Ailes:** Data curation. **Ki Chang:** Methodology, Data curation. **Adam Flanders:** Supervision. **Feroze Mohamed:** Writing – review & editing, Validation, Supervision. **Stavropoula Tjoumakaris:** Writing – review & editing, Validation, Supervision. **Reid Gooch:** Writing – review & editing, Visualization, Conceptualization. **Pascal Jabbour:** Supervision, Conceptualization. **Robert Rosenwasser:** Supervision, Conceptualization. **Mahdi Alizadeh:** Writing – review & editing, Data curation, Conceptualization.

Declaration of competing interest

The authors declare that they have no known competing financial interests or personal relationships that could have appeared to influence the work reported in this paper.

Data availability

Data will be made available on request.

References

- Abbott, N.J., Ronnback, L., Hansson, E., 2006. Astrocyte-endothelial interactions at the blood-brain barrier. *Nat. Rev. Neurosci.* <https://doi.org/10.1038/nrn1824>.
- Andrews, C.E., Mouchtouris, N., Fitchett, E.M., et al., 2019. Revascularization and functional outcomes after mechanical thrombectomy for acute ischemic stroke in elderly patients. *J. Neurosurg.* <https://doi.org/10.3171/2018.12.JNS182399>.

- Arba, F., Rinaldi, C., Caimano, D., et al., 2021. Blood-brain barrier disruption and hemorrhagic transformation in acute ischemic stroke: systematic review and meta-analysis. *Front. Neurol.* <https://doi.org/10.3389/fneur.2020.594613>.
- Berkhemer, O.A., Fransen, P.S.S., Beumer, D., et al., 2015. A randomized trial of intraarterial treatment for acute ischemic stroke. *N. Engl. J. Med.* <https://doi.org/10.1056/NEJMoa1411587>.
- Bernardo-Castro, S., Sousa, J.A., Brás, A., et al., 2020. Pathophysiology of blood-brain barrier permeability throughout the different stages of ischemic stroke and its implication on hemorrhagic transformation and recovery. *Front. Neurol.* <https://doi.org/10.3389/fneur.2020.594672>.
- Costalat, V., Jovin, T.G., Albuquer, J.F., et al., 2024. Trial of thrombectomy for stroke with a large infarct of unrestricted size. *N. Engl. J. Med.* <https://doi.org/10.1056/NEJMoa2314063>.
- Datta, A., Sarmah, D., Kaur, H., et al., 2022. Post-stroke Impairment of the blood-brain barrier and perifocal vasogenic edema is alleviated by endovascular mesenchymal stem cell administration: modulation of the PKCdelta/MMP9/AQP4-Mediated pathway. *Mol. Neurobiol.* <https://doi.org/10.1007/s12035-022-02761-2>.
- Fiorelli, M., Bastianello, S., von Kummer, R., et al., 1999. Hemorrhagic transformation within 36 hours of a cerebral infarct: relationships with early clinical deterioration and 3-month outcome in the European Cooperative Acute Stroke Study I (ECASS I) cohort. *Stroke.* <https://doi.org/10.1161/01.str.30.11.2280>.
- Ford, J.N., Zhang, Q., Sweeney, E.M., et al., 2022. Quantitative water permeability mapping of blood-brain-barrier dysfunction in aging. *Front. Aging Neurosci.* <https://doi.org/10.3389/fnagi.2022.867452>.
- Grefkes, C., Fink, G.R., 2020. Recovery from stroke: current concepts and future perspectives. *Neurol. Res. Pract.* <https://doi.org/10.1186/s42466-020-00060-6>.
- Howarth, C., 2014. The contribution of astrocytes to the regulation of cerebral blood flow. *Front. Neurosci.* <https://doi.org/10.3389/fnins.2014.00103>.
- Huang, X., Yang, Q., Shi, X., et al., 2019. Predictors of malignant brain edema after mechanical thrombectomy for acute ischemic stroke. *J. Neurointerv. Surg.* <https://doi.org/10.1136/neurintsurg-2018-014650>.
- Jenkinson, M., Bannister, P., Brady, M., et al., 2002. Improved optimization for the robust and accurate linear registration and motion correction of brain images. *Neuroimage.* [https://doi.org/10.1016/s1053-8119\(02\)91132-8](https://doi.org/10.1016/s1053-8119(02)91132-8).
- Ling, C., Zhang, J., Shao, X., et al., 2023. Diffusion prepared pseudo-continuous arterial spin labeling reveals blood-brain barrier dysfunction in patients with CADASIL. *Eur. Radiol.* <https://doi.org/10.1007/s00330-023-09652-7>.
- Menon, B.K., Hill, M.D., Davalos, A., et al., 2019. Efficacy of endovascular thrombectomy in patients with M2 segment middle cerebral artery occlusions: meta-analysis of data from the HERMES Collaboration. *J. Neurointerv. Surg.* <https://doi.org/10.1136/neurintsurg-2018-014678>.
- Mo, Y., Sun, Y., Liu, K., 2020. Autophagy and inflammation in ischemic stroke. *Neural Regen. Res.* <https://doi.org/10.4103/1673-5374.274331>.
- Mouchtouris, N., Al Saiegh, F., Fitchett, E., et al., 2019. Revascularization and functional outcomes after mechanical thrombectomy: an update to key metrics. *J. Neurosurg.* <https://doi.org/10.3171/2019.6.JNS183649>.
- Mouchtouris, N., Ailes, I., Gooch, R., et al., 2024. Quantifying blood-brain barrier permeability in patients with ischemic stroke using non-contrast MRI. *Magn. Reson. Imaging.* <https://doi.org/10.1016/j.mri.2024.03.027>.
- Nogueira, R.G., Jadhav, A.P., Haussen, D.C., et al., 2018. Thrombectomy 6 to 24 Hours after Stroke with a Mismatch between Deficit and Infarct. *N. Engl. J. Med.* <https://doi.org/10.1056/NEJMoa1706442>.
- Qureshi, A.I., 2008. Acute hypertensive response in patients with stroke: pathophysiology and management. *Circulation.* <https://doi.org/10.1161/CIRCULATIONAHA.107.723874>.
- Ribeiro, M.C., Hirt, L., Bogousslavsky, J., et al., 2006. Time course of aquaporin expression after transient focal cerebral ischemia in mice. *J. Neurosci. Res.* <https://doi.org/10.1002/jnr.20819>.
- Rueckert, D., Sonoda, L.I., Hayes, C., et al., 1999. Nonrigid registration using free-form deformations: application to breast MR images. *IEEE Trans. Med. Imaging.* <https://doi.org/10.1109/42.796284>.
- Sandoval, K.E., Witt, K.A., 2008. Blood-brain barrier tight junction permeability and ischemic stroke. *Neurobiol. Dis.* <https://doi.org/10.1016/j.nbd.2008.08.005>.
- Sarraj, A., Hassan, A.E., Abraham, M.G., et al., 2023. Trial of endovascular thrombectomy for large ischemic strokes. *N. Engl. J. Med.* <https://doi.org/10.1056/NEJMoa2214403>.
- Sarvari, S., Moakedi, F., Hone, E., et al., 2020. Mechanisms in blood-brain barrier opening and metabolism-challenged cerebrovascular ischemia with emphasis on ischemic stroke. *Metab. Brain Dis.* <https://doi.org/10.1007/s11011-020-00573-8>.
- Semplicini, A., Maresca, A., Boscolo, G., et al., 2003. Hypertension in acute ischemic stroke: a compensatory mechanism or an additional damaging factor? *Arch. Intern. Med.* <https://doi.org/10.1001/archinte.163.2.211>.
- Shao, X., Ma, S.J., Casey, M., et al., 2019. Mapping water exchange across the blood-brain barrier using 3D diffusion-prepared arterial spin labeled perfusion MRI. *Magn. Reson. Med.* <https://doi.org/10.1002/mrm.27632>.
- Shao, X., Jann, K., Ma, S.J., et al., 2020. Comparison between blood-brain barrier water exchange rate and permeability to gadolinium-based contrast agent in an elderly cohort. *Front. Neurosci.* <https://doi.org/10.3389/fnins.2020.571480>.
- Shao, X., Shou, Q., Felix, K., et al., 2024. Age-related decline in BBB function is more pronounced in males than females. *bioRxiv.* <https://doi.org/10.1101/2024.01.12.575463>.
- Spronk, E., Sykes, G., Falcione, S., et al., 2021. Hemorrhagic transformation in ischemic stroke and the role of inflammation. *Front. Neurol.* <https://doi.org/10.3389/fneur.2021.661955>.
- Strbian, D., Sairanen, T., Meretoja, A., et al., 2011. Patient outcomes from symptomatic intracerebral hemorrhage after stroke thrombolysis. *Neurology.* <https://doi.org/10.1212/WNL.0b013e3182267b8c>.
- Tiwari, Y.V., Lu, J., Shen, Q., et al., 2017. Magnetic resonance imaging of blood-brain barrier permeability in ischemic stroke using diffusion-weighted arterial spin labeling in rats. *J. Cereb. Blood Flow Metab.* <https://doi.org/10.1177/0271678X16673385>.
- Uchida, Y., Kan, H., Sakurai, K., et al., 2022. APOE varepsilon4 dose associates with increased brain iron and beta-amyloid via blood-brain barrier dysfunction. *J. Neurol. Neurosurg. Psychiatry.* <https://doi.org/10.1136/jnnp-2021-328519>.
- Uchida, Y., Kan, H., Sakurai, K., et al., 2023. Contributions of blood-brain barrier imaging to neurovascular unit pathophysiology of Alzheimer's disease and related dementias. *Front. Aging Neurosci.* <https://doi.org/10.3389/fnagi.2023.1111448>.
- Uchida, Y., Kan, H., Furukawa, G., et al., 2023. Relationship between brain iron dynamics and blood-brain barrier function during childhood: a quantitative magnetic resonance imaging study. *Fluids Barriers CNS.* <https://doi.org/10.1186/s12987-023-00464-x>.
- Uchida, Y., Kan, H., Kano, Y., et al., 2024. Longitudinal changes in iron and myelination within ischemic lesions associate with neurological outcomes: A pilot study. *Stroke.* <https://doi.org/10.1161/STROKEAHA.123.044606>.
- Wang, D.J.J., Alger, J.R., Qiao, J.X., et al., 2012. The value of arterial spin-labeled perfusion imaging in acute ischemic stroke: comparison with dynamic susceptibility contrast-enhanced MRI. *Stroke.* <https://doi.org/10.1161/STROKEAHA.111.631929>.
- Wang, Y., Huang, H., He, W., et al., 2021. Association between serum NLRP3 and malignant brain edema in patients with acute ischemic stroke. *BMC Neurol.* <https://doi.org/10.1186/s12883-021-02369-4>.